Timescale of degradation-driven protein level fluctuation in the yeast *Saccharomyces cerevisiae*

Bahareh Mahrou[1, 2, *], Azady Pirhanov[1], Moluk Hadi Alijanvand[3], Yong Ku Cho[1, 4, *], Yong-Jun Shin[1]

[1] Biomedical Engineering Department, University of Connecticut, Storrs, CT 06269, USA

[2] Electrical Engineering Department, University of Connecticut, Storrs, CT 06069, USA

[3] Department of Epidemiology and Biostatistics, School of Health, Shahrekord University of Medical Sciences, Shahrekord, Iran

[4] Chemical and Biomolecular Engineering Department, University of Connecticut, Storrs, CT 06269, USA

*** Corresponding authors:** Bahareh Mahrou, E-mail: bahareh.mahrou@uconn.edu

Yong Ku Cho, E-mail: cho@uconn.edu

Abstract

Generating robust, predictable perturbations in cellular protein levels will advance our understanding of protein function and enable control of physiological outcomes in biotechnology applications. Previous studies have shown that controlling RNA transcription achieves perturbations in protein levels over a timescale of several hours. Here, we demonstrate the potential for harnessing the protein degradation machinery to achieve robust, rapid control of a specific protein level in the yeast *Saccharomyces cerevisiae*. Using a light-driven protein degradation machinery and red fluorescent proteins as reporters, we show that under constant transcriptional induction, repeated triangular fluctuations in protein levels can be generated by controlling the protein degradation rate. Consistent with previous results using transcriptional control, we observed a continuous decrease in the magnitude of fluctuations as the modulation frequency increased, indicating low-pass filtering of input perturbation. However, compared to hour-scale fluctuations observed using transcriptional control, modulating the protein degradation rate enabled five to ten minute-scale fluctuations. Our study demonstrates the potential for repeated control of protein levels by controlling protein degradation rate, at timescales much shorter than that achieved by transcriptional control.

Introduction

Extensive research led to insights on how the dynamics and complexity of intracellular regulatory networks are organized to maintain a cellular response (Huang and Ingber 2000, Goldberg 2007, Huang and Ingber 2007, Vogel and Marcotte 2012, Ciechanover 2017). One form of regulation is protein turnover, which refers to the continual renewal or replacement of intracellular proteins. The output of this process is the steady-state intracellular protein concentration, maintained dynamically by continuous production and degradation. The steady-state shifts in response to extracellular stimuli or pathophysiologic conditions, which cause changes in production or degradation rates (Baracos 2000, Pratt, Petty et al. 2002, Mizushima and Klionsky 2007, Hinkson and Elias 2011, Ciechanover 2017, Kneppers, Langen et al. 2017). A powerful approach for gaining fundamental insights for such complex systems would be a bottom-up approach, in which the protein turnover is controlled using external stimuli.

Although production and degradation both contribute to protein turnover, control strategies have largely focused on gene transcription. Multitude of factors involved in transcriptional regulation and its impact on biology and disease have been well characterized (Hill and Treisman 1995, Tautz 2000, Bintu, Buchler et al. 2005, Lee and Young 2013). Numerous previous studies have demonstrated control of transcription using optical and chemical approaches to modulate protein levels (Bennett, Pang et al. 2008, Milias-Argeitis, Summers et al. 2011, Toettcher, Gong et al. 2011, Uhlendorf, Miermont et al. 2012, Melendez, Patel et al. 2014, Milias-Argeitis, Rullan et al. 2016). On the other hand, the effect of degradation process on protein turnover control has been far less characterized. In nature, regulation of protein levels by modulating the degradation rate have been discovered in several proteins with high importance in physiology and drug

64 development (Hellmann and Estelle 2002, Burger and Seth 2004, Varshavsky 2008). For instance,
65 the tumor suppressor protein p53 is kept on at a low steady-state level by Mdm2 that mediates its
66 turnover through protein degradation (Adams 2003, Zilfou and Lowe 2009, Brady and Attardi
67 2010). Upon DNA damage by γ radiation, the steady-state is perturbed, and p53 turnover exhibits
68 an oscillatory behavior indicating that state transitions are occurring repeatedly (Geva-Zatorsky,
69 Rosenfeld et al. 2006). These examples demonstrate the robustness of regulating degradation rates
70 to control protein levels.

71 A major finding from controlling transcription was the experimental observation of low-
72 pass filtering of transcriptional induction in the yeast *S. cerevisiae* (Bennett, Pang et al. 2008). In
73 this previous study, Bennett and colleagues modulated the transcription rate of a fluorescent
74 protein by controlling the extracellular concentration of glucose (transcriptional repressor) over a
75 constant level of galactose (transcriptional inducer) using a microfluidic system (Bennett, Pang et
76 al. 2008). Protein turnover faithfully responded to slow glucose fluctuations, while being
77 insensitive to high-frequency fluctuations. Such low-pass filtering behavior may be important
78 in preventing distortion of cellular response by high-frequency noise signals from the stochastic
79 intracellular environment.

80 Here we applied a light-activated protein degradation machinery (Renicke, Schuster et al.
81 2013) in *S. cerevisiae* to study the dynamics of protein level fluctuations driven by changes in the
82 degradation rate. In this approach, a reporter protein is fused to a blue light-activated degradation
83 signal (photo-sensitive degron, psd), which represents a protein with controllable degradation rates
84 (**Fig. 1**). We take advantage of the light-controlled degradation machinery to analyze the
85 frequency-dependent fluctuations in protein turnover, induced by varying frequency of light inputs
86 that modulate the protein degradation. Square-wave blue light with varying frequencies was

87 delivered to *S. cerevisiae* cells constitutively expressing psd and Δpsd constructs (**Fig. 1**). Using
88 this system, we observed that upon application of low-frequency square waves of light, the protein
89 concentration oscillates with the same corresponding frequency. When the blue light input
90 frequency increases, the amplitude of oscillation decreases, characteristic of a low-pass filter
91 response. However, compared to previously reported transcriptionally controlled fluctuations, the
92 response to degradation-driven fluctuations was faster, enabling protein fluctuations on the order
93 of 10 minutes. This suggests that compared to controlling gene expression, regulating protein
94 degradation allows a much faster response in protein levels.

95 We applied the system identification approach to model the impact of light-activated
96 degradation on protein turnover. System identification is widely used to study the response of a
97 system under time-varying stimulations to construct models of dynamical systems from the
98 measured input and output data (Ljung 1998). We defined a model for the protein turnover based
99 on system identification to better understand its low-pass filtering characteristics. We modeled the
100 dynamic of protein turnover with protein production and degradation as inputs and protein level
101 as the output. Based on our experimental observation on how the protein level changes under
102 different input fluctuations, we adaptively estimated the model parameters. The estimated model
103 parameters were used for the frequency-domain analysis, which allowed quantitative comparison
104 of degradation driven low-pass filtering to previous transcriptional control results.

105

Figure 1.

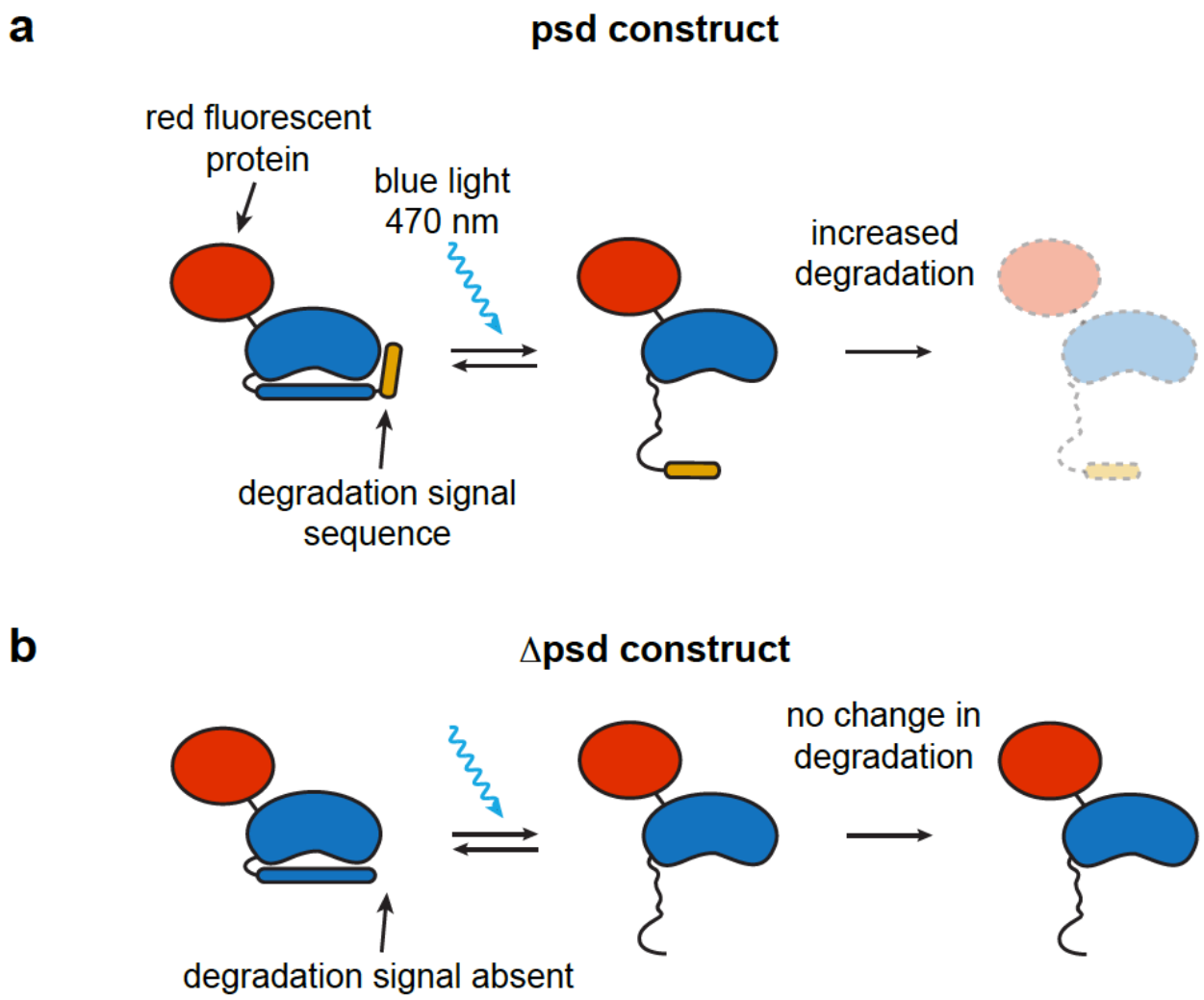

Figure 1. Schematic of photo-sensitive degron (psd) constructs used in this study. In the psd construct (**a**), a protein degradation signal sequence derived from the ornithine decarboxylase is fused to the blue-light sensing light-oxygen-voltage (LOV) domain from *Arabidopsis thaliana*. Upon blue light activation, the degradation signal accessibility increases, resulting in faster protein degradation. The Δpsd construct (**b**), contains all components of psd except the degradation signal sequence.

Results and Discussion

Low-pass filtering of degradation-driven protein level fluctuations in the yeast *S. cerevisiae*

115 The psd module (**Fig. 1**) comprises of light oxygen voltage 2 domain from *Arabidopsis*
116 *thaliana* (*At*LOV2), fused with a derivative of the carboxy-terminal degron of murine ornithine
117 decarboxylase (ODC), enabling the control of ubiquitin-independent proteasomal degradation rate
118 upon blue light illumination (Renicke, Schuster et al. 2013). While *At*LOV2 is sensitive and
119 responsive to blue light, the ODC degradation signal is responsible for increased protein
120 degradation (**Fig. 1**). To observe the effect of fluctuations in protein degradation rate on protein
121 turnover, we applied pulses of blue light and monitored the fluorescence emission from the red
122 fluorescent protein tagRFP fused to psd (**Fig. 1a**). To validate protein degradation due to the ODC
123 degradation signal, we generated a control construct that lacks the signal sequence, termed Δpsd
124 (**Fig. 1b**). The expression of these constructs in yeast *S. cerevisiae* was continuously driven using
125 the constitutive GAL_{1-10} promoter under galactose. To validate continuous expression, we
126 measured the *tagRFP* transcript level by extracting the mRNA from yeast cells and performing a
127 quantitative polymerase chain reaction (qPCR) of the transcript (**Fig. 2a,** see **Supp. Fig. 1** and
128 **Supp. Table 1** for RNA quality control and primers used). We illuminated the cells with maximum
129 blue light intensity used in this study (light power density of 0.027 mW/mm^2 (106.02 $\mu mol/m^2s$))
130 and the longest duration ($1/f$ = 100 min where f indicates illumination frequency) to assess the
131 effect of illumination on gene expression. The mRNA was extracted from cells at the start of the
132 experiment and at the end of each illumination cycle (see inset in **Fig. 2a**). Two primer sets that
133 bind to different regions of *tagRFP* were used for amplification, along with primers for two
134 previously validated housekeeping genes, *TFC1* and *UBC6* (Teste, Duquenne et al. 2009), as a
135 reference. Expression of *tagRFP* remained unchanged for 200 minutes and a significant increase
136 was detected between 200 to 300 minutes (**Fig. 2a**, p = 0.014 and 0.023, student's t-test comparing
137 ΔCt at 200 min. to that at 300 min. for the two *tagRFP* primer sets, respectively (n = 3 independent

138 culture preparations)). This result indicates that the GAL_{1-10} promoter allows continuous

139 expression of the tagRFP constructs, unhindered by light illumination.

140

Figure 2.

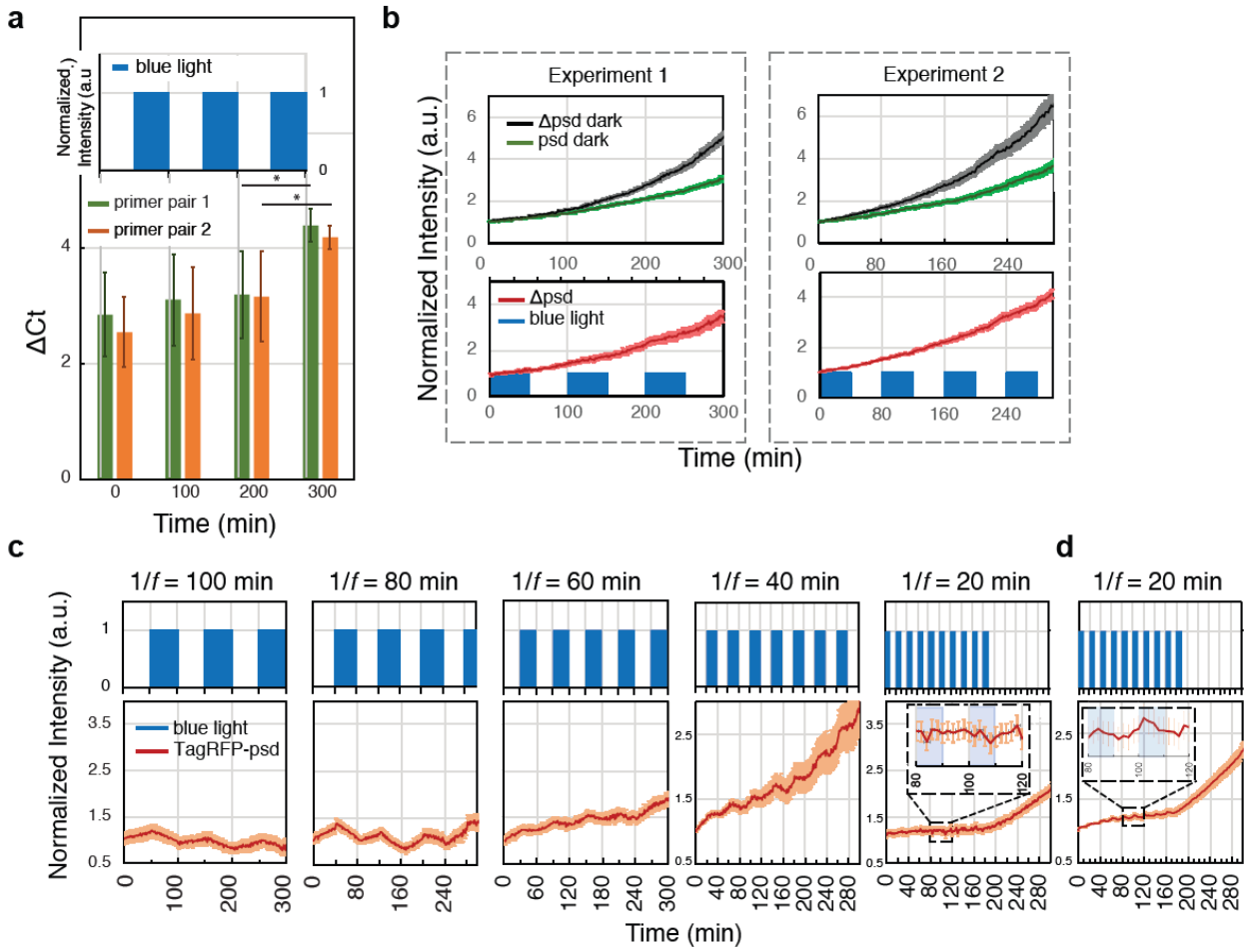

Figure 2. Experimental validation and observation of degradation-driven protein level fluctuations in yeast expressing tagRFP fused to psd or Δpsd. (**a**) qPCR analysis of *tagRFP* transcripts during blue light illumination (inset indicates illumination timepoints). Two sets of primers (primer sets 1 and 2) that bind to different regions of *tagRFP* were used, and previously validated housekeeping genes *TFC1* and *UBC6* were used as references. ΔCt values were calculated by subtracting the Ct of *tagRFP* from the average of the Ct of the two reference genes. *: $p < 0.05$, student's t-test comparing ΔCt at 200 min. to that at 300 min. Error bars indicate standard deviation from n = 3 independent culture preparations. (**b**) Normalized fluorescence level of tagRFP-psd and tagRFP-Δpsd under dark (top panels); tagRFP-Δpsd illuminated with blue light cycles (bottom panels). Solid lines indicate the mean fluorescence intensities and lighter lines indicate standard deviation from n = 10 to 15 colonies of cells. (**c**) Fluorescence of tagRFP-psd under varying frequencies of blue light illumination. *f* denotes the temporal frequency and 1/*f* indicates cycle period. Solid lines indicate the mean fluorescence intensities and lighter lines indicate standard deviation from n = 10 to 15 colonies. (**d**) Experiment for 1/*f* = 20 min. was repeated with 25 colonies of cells. Same intensity of blue light (power density of 0.027 mW/mm^2 (106.02 μmol/m^{2}s)) was used in all panels. In panels (b) and (c), data for each illumination frequency was obtained in separate experiments using independent cultures of cells.

159 Since the cell cycle of *S. cerevisiae* is on the order of 100 min. (Herskowitz 1988), we
160 observed cell division during the repeated illumination cycles (**Supp. Fig. 2**). Proteins in each cell
161 are divided into daughter cells, resulting in dilution of proteins. One approach to quantify the entire
162 amount of proteins throughout cell division is to sum the fluorescence intensity from a colony of
163 cells originating from mother cells (Talia, Skotheim et al. 2007). In agreement with previous
164 studies, we found that summing the fluorescence intensity of a colony of cells results in continuous
165 increase (red line in **Supp. Fig. 2**), while the fluorescence intensity divided by the area of cells
166 fluctuates as the cells divide (blue line in **Supp. Fig. 2**). To capture the change in protein level
167 decoupled from cell division, we used the sum of fluorescence intensities of a colony of cells as a
168 measure of protein levels throughout this study.

169 We then tested the effect of pulses of blue light on yeast cells expressing tagRFP-psd or
170 tagRFP-Δpsd. In the absence of blue light, the normalized fluorescence level of tagRFP-psd and
171 tagRFP-Δpsd (see **Materials and Methods** section for calculation) showed a continuous increase
172 over 300 min. (**Fig. 2b**). The fluorescence level of tagRFP-Δpsd was generally higher than that of
173 tagRFP-psd (**Fig. 2b**), likely due to the fact that the LOV domain conformation is in equilibrium
174 between active and inactive states even under dark (Strickland, Yao et al. 2010), resulting in slight
175 background degradation even without blue illumination. As anticipated, the level of tagRFP-Δpsd
176 was unresponsive to two distinct frequencies of illumination (**Fig. 2b**, $f = 1/100$ mins and $f = 1/80$
177 mins, respectively in experiments 1 and 2). In contrast, fluorescence level of tagRFP-psd showed
178 distinct fluctuations with varying frequency of blue light (**Fig. 2c**). We repeated the experiment 5
179 times, each at a distinct illumination frequency (**Fig. 2c**). Fluctuation in protein level was clearly
180 visible up to illumination frequency of $1/f = 40$ mins, but not at the highest illumination frequency
181 tested ($1/f = 20$ mins) (**Fig. 2c**). When the experiment for $1/f = 20$ mins was repeated with a larger

182 number of colonies cells, the fluctuation was discernable albeit markedly reduced (**Fig. 2d**). Based
183 on these findings, we conclude that the output fluctuations observed in the experiment are the
184 result of light-induced increase in protein degradation rate mediated by the psd.

185 The reduction in fluctuations in protein levels at higher input illumination frequency is
186 characteristic of low-pass filtering (Antoniou 2016), and indicate that the input perturbation
187 driving protein degradation has been filtered out at these higher frequencies. To analyze the low-
188 pass behavior of the degradation driven protein turnover, we determined the time delay between
189 the input blue light illumination frequency and output protein fluorescence intensity using cross-
190 correlation. We calculated the cross-correlation (see **Supplementary Information** for calculation)
191 for experiments using tagRFP-psd shown in **Fig. 2c**. Since the protein level decreases upon
192 illumination, a minimum in the cross-correlation occurs (**Fig. 3**, indicated by arrows). Based on
193 the minimum value for each experiment, the time delay between the input and output signals
194 ranged from 1 to 15 minutes (see **Supplementary Information** for calculation). We find that the
195 time at which minima occur shortens as the input frequency fluctuations increases, characteristic
196 of a low-pass filtering system.

197

Figure 3.

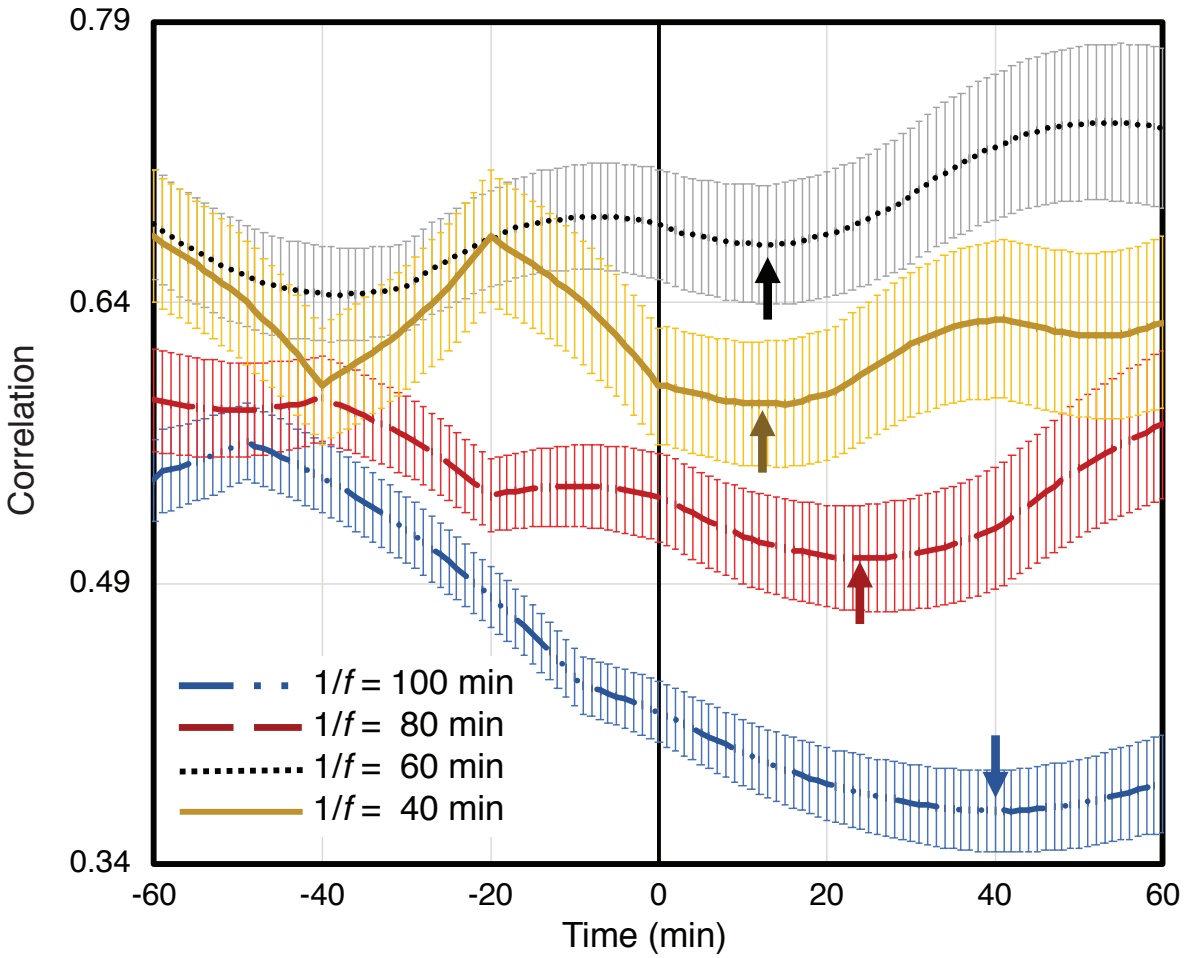

Figure 3. Cross-correlation between input blue light illumination and protein fluorescence intensity. The curves are cross-correlations resulted from four experiments with varying input frequencies indicated in the inset. The arrows show the minimum (after time 0) of each curve. Note that the minimums do not directly indicate the time delay, but allow the calculation of the time delay as shown in the Supplementary Information.

Degradation-driven fluctuations in a faster maturing fluorescent protein.

Fluorescent proteins contain a chromophore formed through autocatalytic maturation (Wachter 2007, Craggs 2009, Subach and Verkhusha 2012). The fluorescence is only detected after maturation, effectively causing a slowdown of apparent protein production rate. Although not tested, a shift in protein maturation time is expected to impact the low-pass filtering behavior

210 when transcription rate is modulated as in Bennett *et al.*'s work (Bennett, Pang et al. 2008). In
211 contrast, when protein degradation rate is modulated, as in our experiments, a shift in protein
212 maturation time should not affect the low-pass filtering behavior.

213 To test this, we replaced tagRFP in tagRFP-psd with the fluorescent protein mCherry
214 (mCherry-psd), which has a significantly shorter maturation time compared to that of tagRFP
215 (maturation half-time of ~40 minutes for mCherry vs. ~100 minutes for TagRFP (Merzlyak,
216 Goedhart et al. 2007)). We then repeated the experiment shown in **Fig. 2c** using mCherry-psd and
217 monitored the mCherry fluorescence in colony numbers similar to that in **Fig. 2d** (25 to 30 colonies
218 having 4 to 8 cells at the beginning of the experiment). Clear fluctuations in mCherry fluorescence
219 were visible, down to illumination frequency of $1/f = 20$ min (**Fig. 4a**). We also conducted more
220 experiments with higher frequencies of input ($1/f = 10$ min and $1/f = 5$ min) and detected small but
221 distinguishable fluctuations (**Fig. 4b** and see **Supp. Fig. 4** for extended experiments). We observed
222 consistent decrease in the amplitude of output fluctuations upon increasing the frequency of
223 degradation fluctuation, characteristic of a low-pass filtering behavior.

224

Figure 4.

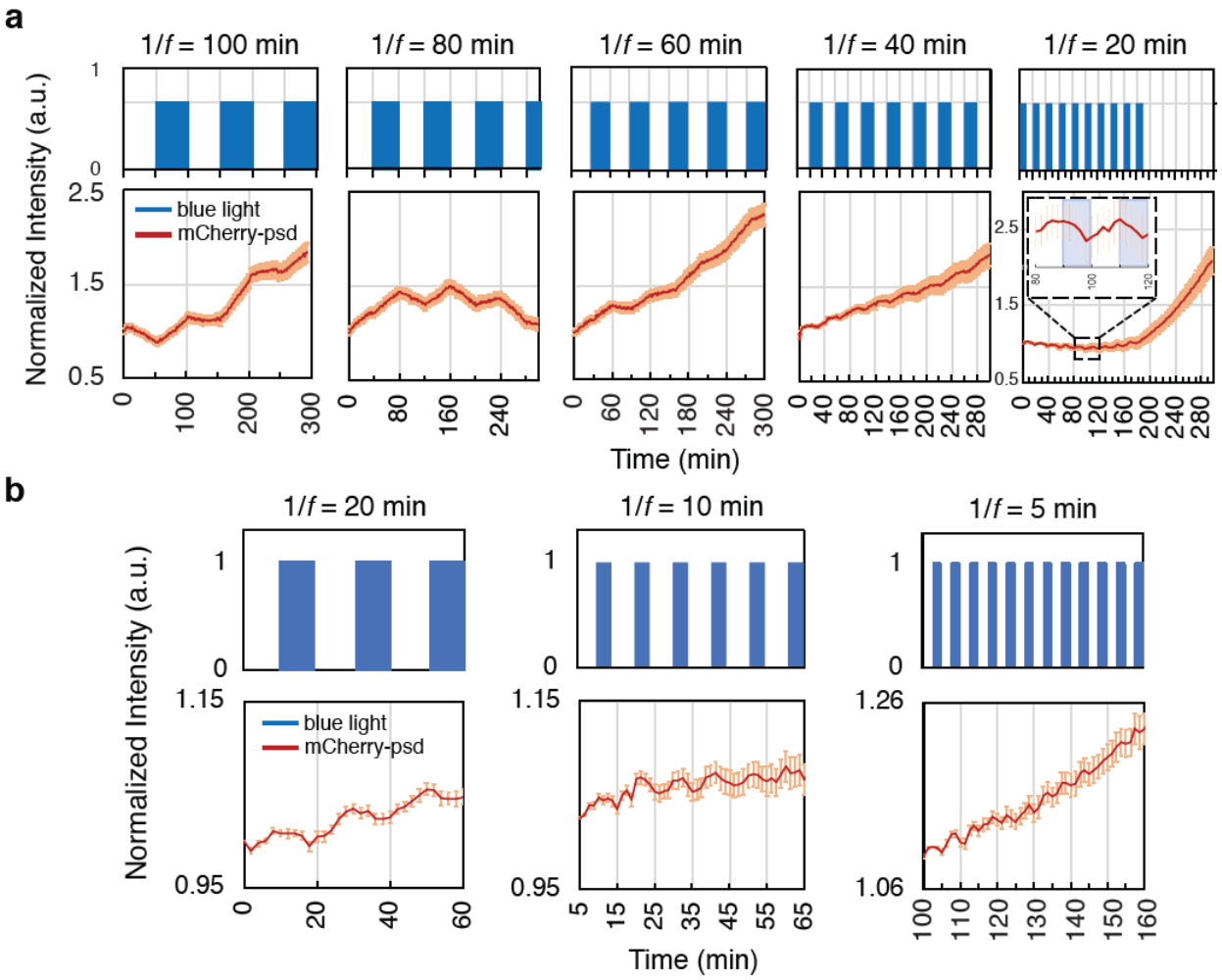

Figure 4. Experimental observation of degradation-driven protein level fluctuations in yeast expressing mCherry fused to psd. (**a**) Fluorescence of mCherry-psd under varying frequencies of blue light illumination. (**b**) Fluorescence of mCherry-psd under higher frequency illumination. For frequency $1/f$ = 20 min., experiment in panel (a) was repeated. For all panels, solid lines indicate the mean fluorescence intensities and lighter lines indicate standard deviation from n = 25 to 30 colonies. Blue light intensity was 0.027 mW/mm^2 (106.02 μmol/m^{2}s)) for all panels.

System identification and frequency-domain analysis.

To quantitatively assess the low-pass filtering, we constructed a mathematical model for degradation-driven protein turnover using the difference equation approach we previously described (Shin 2016). The model equation can be expressed as:

$$y(n) = p_y y(n-1) + p_{pro} u_{pro}(n-1) + p_{deg} u_{deg}(n-1) \quad (1)$$

where n is the discrete-time index, y(n) is the normalized fluorescence intensity at time n, $u_{pro}(n)$ is the normalized amount of galactose (transcription inducer) at time n, $u_{deg}(n)$ is the normalized intensity of blue light (degradation rate controller) at time n. Parameters p_y, p_{pro}, and p_{deg} indicate endogenous degradation, production, and light-induced degradation, respectively. These parameters can be adaptively estimated from the experimental data using the normalized least mean square (NLMS) algorithm, one of commonly used adaptive system identification algorithms (Sayed 2011). Assuming constant protein production, as indicated by relatively consistent transcription (**Fig. 2a**), eq. 1 can be simplified by approximating $u_{pro}(n)$ to 1:

$$y(n) = p_y y(n-1) + p_{pro} + p_{deg} u_{deg}(n-1) \quad (2)$$

The above equation represents a multiple-input single-output (MISO) system that can be transformed into the frequency domain using the z–transform.

$$Y(z) = \frac{p_{deg}}{z-p_y} U_{deg}(z) + \frac{p_{pro} z^2}{(z-1)(z-p_y)} \quad (3)$$

Eq. 3 illustrates the relationship between the single output Y(z) and two independent inputs (blue light intensity, $U_{deg}(z)$, and the normalized galactose concentration which is assumed to be constant at 1). The equation can be re-expressed in matrix form:

$$Y(z) = \begin{bmatrix} \frac{p_{deg}}{z-p_y} & \frac{p_{pro} z^2}{(z-1)(z-p_y)} \end{bmatrix} \begin{bmatrix} U_{deg}(z) \\ 1 \end{bmatrix} = [H_1(z) \quad H_2(z)] \begin{bmatrix} U(z) \\ 1 \end{bmatrix} \quad (4)$$

$$H_1(z) = \frac{p_{deg}}{z-p_y} \quad (5)$$

$$H_2(z) = \frac{p_{pro} z^2}{(z-1)(z-p_y)} \quad (6)$$

256 where $H_1(z)$ shows the relationship between the output Y(z) (protein fluorescence intensity) and
257 input $U_{deg}(z)$ (blue light intensity). The unknown parameter values p_y and p_{deg} in $H_1(z)$ were
258 estimated using the NLMS adaptive system identification algorithm (See **Supplementary**
259 **Information** and **Supp. Fig. 5**). The Bode plot in **Fig. 5** (indicated as 'Model') shows the
260 amplitude and phase shift response of $H_1(z)$, calculated based on the mean and standard deviation
261 of estimated parameter values acquired from each experiment (See **Supplementary Information**).
262 The amplitude responses clearly show low-pass filtering, indicated by a steady decrease in the
263 amplitude of the fluctuations as input blue light illumination frequency increases (**Fig. 5a**). We
264 performed a statistical comparison of experimental results (tagRFP-psd vs. mCherry-psd) as well
265 as experiments to the model (tagRFP-psd vs. model, mCherry-psd vs. model). The summary of
266 statistical comparisons in **Table 1** show that the model captured the amplitude and phase shift
267 responses well. As for amplitude response, no significant difference was found when comparing
268 model vs. tagRFP-psd as well as model vs. mCherry-psd (**Fig. 5a** and **Table 1**). When comparing
269 phase shift response of model vs. tagRFP-psd, significant difference was found only for at $1/f =$
270 100 min and $1/f = 80$ min, but not at other frequencies (**Fig. 5b** and **Table 1**). Phase shift response
271 of model vs. mCherry-psd was not significantly different at all illumination frequencies (**Fig. 5b**
272 and **Table 1**). When comparing tagRFP-psd vs. mCherry-psd, mCherry-psd showed significantly
273 smaller amplitude response at frequencies $1/f = 80$ min, $1/f = 60$ min, and $1/f = 40$ min (**Fig. 5a**
274 and **Table 1**), but no significant difference was found for phase shift (**Fig. 5b** and **Table 1**). These
275 results show that both tagRFP-psd and mCherry-psd showed low-pass filtering with similar time
276 delay, and confirm that the difference in maturation time between tagRFP and mCherry do not
277 cause a change in the low-pass filtering behavior. Comparing the Bode plot of our experiments
278 with the previous study using transcriptional control (Bennett, Pang et al. 2008), we found that the

279 same amplitude of fluctuations (e.g., an amplitude of around 0.3 which is equivalent to -10.5 dB)
280 was achieved at approximately 3-fold higher frequencies (0.06 rad/min) in degradation-driven
281 control (achieved at frequency of 0.02 rad/min), indicating a much faster timescale. Taken
282 together, these results demonstrate that degradation driven control is a robust approach for
283 controlling protein levels at minutes timescale.

284 Although we demonstrated this capability in the yeast *S. cerevisiae*, we anticipate the
285 timescale determined here will apply to many other cell types, considering the UPS is widely
286 conserved among eukaryotes. In fact, light-sensitive degradation using the psd has been
287 successfully demonstrated in cell types including human, and other mammalian cells (Sun, Zhang
288 et al. 2017, Baaske, Gonschorek et al. 2018). Moreover, light-activation is highly suitable for
289 feedback control since the intensity, frequency, and location of illumination can be instantly
290 modulated. Since we demonstrated that controlling the degradation rate is sufficient to drive
291 protein levels under constant transcription, we anticipate this approach to allow generating protein
292 oscillations previously not achievable using transcriptional control.

293

Figure 5.

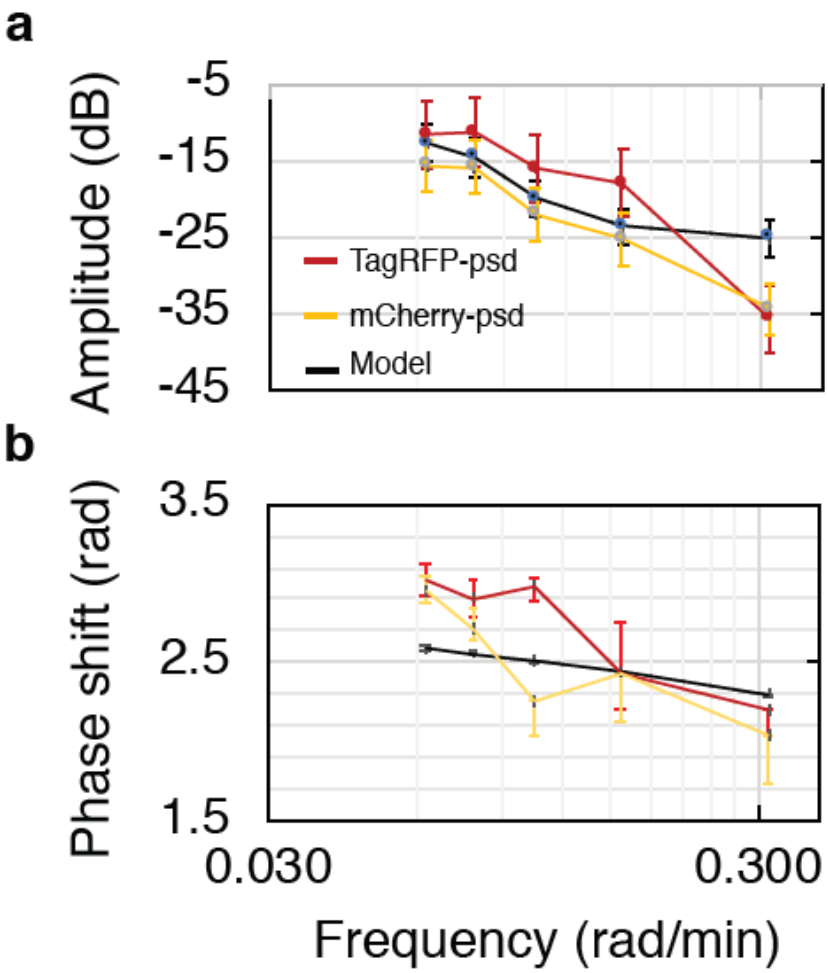

Figure 5. Model and experimental comparison of low-pass filtering using Bode plots. (**a**) Amplitude response and (**b**) phase shift response from tagRFP-psd, mCherry-psd, and model calculations as a function of input frequency. Data points indicate median and error bars indicate interquartile range (IQR) from four colonies of cells. Statistical analysis of the results is found in Table 1.

Table 1.

Group \ Set	f = 2π/100 (1/f = 100 min)		f = 2π/80 (1/f = 80 min)		f = 2π/60 (1/f = 60 min)		f = 2π/40 (1/f = 40 min)		f = 2π/20 (1/f = 20 min)	
	Amplitude	Phase shift	Amplitude	Phase shift	Amplitude	Phase shift	Amplitude	Phase shift	Amplitude	Phase shift
	Median (IQR)									
Model	-12.691 (3.352)	2.586 (0.027)	-14.579 (4.359)	2.554 (0.030)	-20.007 (4.805)	2.510 (0.008)	-23.572 (4.840)	2.444 (0.010)	-25.096 (4.847)	2.300 (0.016)
tagRFP-psd	-11.537 (0.642)	3.016 (0.204)	-11.293 (0.288)	2.906 (0.236)	-16.055 (0.440)	2.985 (0.157)	-17.9937 (0.446)	2.435 (0.550)	-35.654 (0.446)	2.199 (0.471)
mCherry-psd	-15.686 (2.608)	2.953 (0.173)	-15.935 (1.590)	2.710 (0.196)	-22.007 (3.538)	2.251 (0.209)	-25.2071 (4.433)	2.435 (0.314)	-34.437 (4.433)	2.042 (0.314)
P-value	0.095	0.024*	0.023*	0.030*	0.024*	0.115	0.023*	0.981	0.351	0.701

*Difference in median value of model, tagRFP-psd, and mCherry-psd assessed using Kruskal-Wallis test, P-value < 0.05

Gray highlighted cells in each column indicate pairs with significant difference as assessed using NEMENYI test for multiple pairwise comparisons between the groups, P-value < 0.05

306

307 Conclusions

308 Here we demonstrated robust generation of controlled protein level fluctuations in the yeast *S.*
309 *cerevisiae* using a blue-light induced protein degradation machinery. We found that by monitoring
310 the total fluorescence of colonies of cells, protein fluctuations with minutes timescale can be
311 reproducibly generated. By using two red fluorescent proteins with distinct maturation time, we
312 show that the delay in protein production rate does not change the protein level fluctuation
313 generated by modulating the protein degradation rate. The results show that controlling protein
314 degradation rates under constant transcription as a means for modulating protein levels,
315 demonstrating a clear pathway for feedback control of protein levels with minutes timescale.

316

317 Materials and Methods

318 **Cloning and expression of a photo-sensitive degron in yeast**

319 The photo-sensitive degron (psd) module used in this study has been previously described by
320 Renicke and colleagues (Renicke, Schuster et al. 2013). A red fluorescent reporter protein
321 (tagRFP) was fused to the N-terminus of *At*LOV2. The tagRFP-psd construct was cloned into the
322 pRS316 plasmid (Huang and Shusta 2005) (a gift from Dr. Eric Shusta) using restriction enzymes
323 NotI and BsrGI (New England Biolabs) under the galactose inducible $GAL_{1\text{-}10}$ promoter. Psd
324 without the ODC degron (Δpsd) was generated using polymerase chain reaction and cloned using
325 the same restriction sites. The resulting plasmids were named pRS316-tagRFP-psd and pRS316-
326 tagRFP-Δpsd respectively. The plasmids were transformed into the yeast *Saccharomyces*

327 *cerevisiae* strain BJ5464 (BJα, α *ura3-52 trp1 leu2Δ1 his3Δ200 pep4:: HIS3 prb1Δ1.6R can1*
328 *GAL*) cells, using a commercially available kit (Zymo Research). Transformed cells were grown
329 in SD-CAA medium (0.1 M sodium phosphate, pH 6.0, 6.7 g/L yeast nitrogen base, 5.0 g/L
330 casamino acids, 20.0 g/L glucose), supplemented with tryptophan (0.04 g/L) at 30 ºC on an orbital
331 shaker (250 rpm).

332 **qPCR gene expression analysis**

333 Briefly, cells containing pRS316-tagRFP-Δpsd plasmid were grown in SD-CAA medium
334 supplemented with tryptophan (0.04 g/L) at 30 ºC on an orbital shaker (250 rpm) overnight. Yeast
335 cells grown overnight were diluted to OD_{600} of 1, and the medium was replaced with the induction
336 medium, SG-CAA (0.1 M sodium phosphate, pH 6.0, 6.7 g/L yeast nitrogen base, 5.0 g/L casamino
337 acids, 20.0 g/L galactose) supplemented with tryptophan (0.04 g/L) and incubated at 16 ºC on an
338 orbital shaker (250 rpm) for 20 hrs. Then cells were diluted 5-fold in SG-CAA (supplemented with
339 tryptophan) and grown at 30 ºC on an orbital shaker (250 rpm) for period of 400 mins with blue
340 light illumination with period of $1/f$ = 100 mins. Cells (10 mL of culture) were collected at the
341 end of each 100 min illumination cycle (blue light power density of 0.027 mW/mm^2 (106.02
342 $\mu mol/m^2s$)), and stored at 4 ºC until analysis. RNA extraction was performed right after samples
343 collecting samplesusing RNeasy Mini Kit (Qiagen cat# 74104) according to manufacturer's
344 protocols. Quality of purified RNAs were checked by measuring the ratio of absorbance at 260 nm
345 to 280 nm (A260/A280) by using the NanoDrop ND-1000 (Nanodrop Technologies). Integrity and
346 concentration of RNA were assessed by using the automated electrophoresis station Agilent
347 Tapestation 4200 (Bio-Rad).

348 All RNA samples were diluted in RNase/DNase free water (Fisher Scientific cat# BP28191)) at
349 the same concentration and a volume corresponding to 500 ng was added to iScript™ cDNA
350 synthesis kit reagents (Bio-Rad cat# 1708890) for cDNA synthesis, per kit instructions. The
351 reaction mix was incubated for 5 min at 25 °C, followed by 30 min at 46 °C and 5 min at 95 °C
352 and hold at 4 °C. The cDNA samples were then stored at –80 °C.

353 qPCR was performed by using SsoAdvanced™ Universal SYBR Green Supermix (Bio-Rad cat#
354 1725270). 2 µl of cDNA was used per total of 20 µl reaction mixture as a template. *TFC1* and
355 *UBC6* genes were used as housekeeping genes. See Supplementary Fig. 1 and Table 1 for RNA
356 quality control and primers used. Cycling conditions included a polymerase activation step of 98°C
357 for 2 min and 40 cycles of 98°C for 2 sec and annealing /extension at 60°C for 5 sec followed by
358 melt curve analysis from 65 to 95°C in 0.5°C increments. Size of amplicons for each gene were
359 verified on a 2% agarose gel. ΔCt values were calculated by subtracting the threshold cycle (Ct)
360 of *tagRFP* from the average of the Ct of the two reference genes.

361 **Light-induced degradation and imaging**

362 Yeast cells grown overnight were diluted to OD_{600} of 1, and the medium was replaced with the
363 induction medium, SG-CAA (0.1 M sodium phosphate, pH 6.0, 6.7 g/L yeast nitrogen base, 5.0
364 g/L casamino acids, 20.0 g/L galactose) supplemented with tryptophan (0.04 g/L) at 16 ºC on an
365 orbital shaker (250 rpm) for 20 hrs. Cells were kept in the dark during the entire induction period
366 to prevent unwanted degradation. To activate degradation, blue light (470 nm) was delivered at a
367 power density of 0.027 mW/mm^2 (106.02 $\mu mol/m^2s$) using a light emitting diode (LED, Thorlabs).
368 For imaging tagRFP, green light (530 nm) was delivered at a power density of 0.69 mW/mm^2.

369 Extra precautions were taken to prevent exposure to light after induction until the
370 experiment was completed. For imaging, cells were put into 96 wells plates coated with
371 Concanavalin A (2 mg/mL, Sigma Aldrich) to attach the cells to the bottom of plates. Unbound
372 cells were washed with SG-CAA medium.

373 To quantify the protein level, the sum of fluorescence intensity of each colony was
374 measured over the experiment. To identify regions with colonies, 'Otsu dark' auto threshold
375 method in ImageJ library was used. The mean fluorescence intensity over all colonies of all 5
376 experiments is defined as the normalization factor. The sum for each colony was then normalized
377 to the normalization factor. Additionally, an offset specific to each experiment is used in all
378 experiments' dataset so that the first value starts at a normalized value of 1. In each experiment,
379 measurements from at least 10 colonies were recorded and averaged.

380 LED intensities were controlled by an Arduino (See **Supplementary Information**)
381 controlled using the µManager (Edelstein, Tsuchida et al. 2014). The system snaps images from
382 all samples every minute while exposing psd and Δpsd samples to blue LED controlled via the
383 Java programming language (See Supplementary Information). The image processing/analysis
384 was done using the imageJ/µManager libraries (See **Supplementary Information** for more details
385 and the codes are available in Github (Mahrou 2021)).

386 **Statistical analysis**

387 To generate the Bode plot, the median phase and amplitude values from each of the 5
388 frequencies from 4 colonies of cells and median of 4 parameter values estimated for the model
389 were calculated. The median values between the three datasets (Model, tagRFP-psd, and mCherry-
390 psd) were compared using the Kruskal-Wallis test. When the median differences between the

391 groups were statistically significant (P-value<0.05), the NEMENYI test was also used to compare
392 the median differences between groups of two. Statistical analyses were performed using real
393 statistics in excel (Charles Zaiontz, www.real-statistics.com).

394

395 Acknowledgements

396 This work was funded by the University of Connecticut, the Alzheimer's Association (2019-
397 AARG-NTF-640971), and NIH (1R21NS111358-01A1). We thank Bo Reese and Lu Li of Center
398 for Genome Innovation within the Institute for Systems Genomics at the University of Connecticut
399 for their help in the RNA quality assessment and qPCR analysis. The authors declare that they
400 have no conflicts of interest with the contents of this article.

401 Author Contributions

402 B.M. designed and performed the experiments, derived the model and analyzed the data. A.P.
403 cloned the psd constructs and conducted the qPCR gene expression analysis. M.H. conducted the
404 statistical analysis. Y.C. and Y.S. supervised the project and assisted with the analysis and the
405 interpretation of data and model. All authors discussed the results and contributed to the
406 manuscript.

407

408

References

Adams, J. (2003). "Potential for proteasome inhibition in the treatment of cancer." Drug discovery today **8**(7): 307-315

Antoniou, A. (2016). Digital signal processing, McGraw-Hill.

Baaske, J., P. Gonschorek, R. Engesser, A. Dominguez-Monedero, K. Raute, P. Fischbach, K. Muller, E. Cachat, W. W. A. Schamel, S. Minguet, J. A. Davies, J. Timmer, W. Weber and M. D. Zurbriggen (2018). "Dual-controlled optogenetic system for the rapid down-regulation of protein levels in mammalian cells." Sci Rep **8**(1): 15024.10.1038/s41598-018-32929-7

Baracos, V. E. (2000). "Regulation of skeletal-muscle–protein turnover in cancer-associated cachexia." Nutrition **16**(10): 1015-1018

Bennett, M. R., W. L. Pang, N. A. Ostroff, B. L. Baumgartner, S. Nayak, L. S. Tsimring and J. Hasty (2008). "Metabolic gene regulation in a dynamically changing environment." Nature **454**(7208): 1119

Bintu, L., N. E. Buchler, H. G. Garcia, U. Gerland, T. Hwa, J. Kondev and R. Phillips (2005). "Transcriptional regulation by the numbers: models." Current opinion in genetics & development **15**(2): 116-124

Brady, C. A. and L. D. Attardi (2010). "p53 at a glance." J Cell Sci **123**(15): 2527-2532

Burger, A. M. and A. K. Seth (2004). "The ubiquitin-mediated protein degradation pathway in cancer: therapeutic implications." European journal of cancer **40**(15): 2217-2229

Ciechanover, A. (2017). "Intracellular protein degradation: from a vague idea thru the lysosome and the ubiquitin-proteasome system and onto human diseases and drug targeting." Best Practice & Research Clinical Haematology **30**(4): 341-355

Craggs, T. D. (2009). "Green fluorescent protein: structure, folding and chromophore maturation." Chemical Society Reviews **38**(10): 2865-2875

Edelstein, A. D., M. A. Tsuchida, N. Amodaj, H. Pinkard, R. D. Vale and N. Stuurman (2014). "Advanced methods of microscope control using μManager software." Journal of Biological Methods **1**(2): e10.10.14440/jbm.2014.36

Geva-Zatorsky, N., N. Rosenfeld, S. Itzkovitz, R. Milo, A. Sigal, E. Dekel, T. Yarnitzky, Y. Liron, P. Polak and G. Lahav (2006). "Oscillations and variability in the p53 system." Molecular systems biology **2**(1)

Goldberg, A. (2007). "Functions of the proteasome: from protein degradation and immune surveillance to cancer therapy." Biochemical Society Transactions **35**(1): 12-17

Hellmann, H. and M. Estelle (2002). "Plant development: regulation by protein degradation." science **297**(5582): 793-797

Herskowitz, I. (1988). "Life cycle of the budding yeast Saccharomyces cerevisiae." Microbiol Rev **52**(4): 536-553.10.1128/mr.52.4.536-553.1988

443 Hill, C. S. and R. Treisman (1995). "Transcriptional Regulation by Extracellular signals: Mechanisms and
444 Specificity." Cell **80**(2): 199-211.https://doi.org/10.1016/0092-8674(95)90403-4

445 Hinkson, I. V. and J. E. Elias (2011). "The dynamic state of protein turnover: It's about time." Trends in
446 cell biology **21**(5): 293-303

447 Huang, D. and E. V. Shusta (2005). "Secretion and surface display of green fluorescent protein using the
448 yeast Saccharomyces cerevisiae." Biotechnol Prog **21**(2): 349-357.10.1021/bp0497482

449 Huang, S. and D. E. Ingber (2000). "Shape-dependent control of cell growth, differentiation, and apoptosis:
450 switching between attractors in cell regulatory networks." Experimental cell research **261**(1): 91-103

451 Huang, S. and D. E. Ingber (2007). "A non-genetic basis for cancer progression and metastasis: self-
452 organizing attractors in cell regulatory networks." Breast disease **26**(1): 27-54

453 Kneppers, A. E., R. C. Langen, H. R. Gosker, L. B. Verdijk, N. C. Lipovec, P. A. Leermakers, M. C.
454 Kelders, C. C. de Theije, D. Omersa and M. Lainscak (2017). "Increased Myogenic and Protein Turnover
455 Signaling in Skeletal Muscle of Chronic Obstructive Pulmonary Disease Patients With Sarcopenia." Journal
456 of the American Medical Directors Association **18**(7): 637. e631-637. e611

457 Lee, T. I. and R. A. Young (2013). "Transcriptional regulation and its misregulation in disease." Cell
458 **152**(6): 1237-1251

459 Ljung, L. (1998). System identification. Signal analysis and prediction, Springer**:** 163-173.

460 Mahrou, B. (2021). "Degradation driven protein turnover." from https://github.com/Bam12006/The-low-
461 pass-filtering-effect-of-degradation-driven-protein-turnover.

462 Melendez, J., M. Patel, B. L. Oakes, P. Xu, P. Morton and M. N. McClean (2014). "Real-time optogenetic
463 control of intracellular protein concentration in microbial cell cultures." Integrative Biology **6**(3): 366-372

464 Merzlyak, E. M., J. Goedhart, D. Shcherbo, M. E. Bulina, A. S. Shcheglov, A. F. Fradkov, A. Gaintzeva,
465 K. A. Lukyanov, S. Lukyanov and T. W. Gadella (2007). "Bright monomeric red fluorescent protein with
466 an extended fluorescence lifetime." Nature methods **4**(7): 555

467 Milias-Argeitis, A., M. Rullan, S. K. Aoki, P. Buchmann and M. Khammash (2016). "Automated
468 optogenetic feedback control for precise and robust regulation of gene expression and cell growth." Nature
469 communications **7**: 12546

470 Milias-Argeitis, A., S. Summers, J. Stewart-Ornstein, I. Zuleta, D. Pincus, H. El-Samad, M. Khammash
471 and J. Lygeros (2011). "In silico feedback for in vivo regulation of a gene expression circuit." Nature
472 biotechnology **29**(12): 1114

473 Mizushima, N. and D. J. Klionsky (2007). "Protein turnover via autophagy: implications for metabolism."
474 Annu. Rev. Nutr. **27**: 19-40

475 Pratt, J. M., J. Petty, I. Riba-Garcia, D. H. Robertson, S. J. Gaskell, S. G. Oliver and R. J. Beynon (2002).
476 "Dynamics of protein turnover, a missing dimension in proteomics." Molecular & Cellular Proteomics **1**(8):
477 579-591

478 Renicke, C., D. Schuster, S. Usherenko, L.-O. Essen and C. Taxis (2013). "A LOV2 domain-based
479 optogenetic tool to control protein degradation and cellular function." Chemistry & biology **20**(4): 619-626

480 Sayed, A. H. (2011). Adaptive filters, John Wiley & Sons.

481 Shin, Y.-J. (2016). "Digital Signal Processing and Control for the Study of Gene Networks." Scientific
482 reports **6**: 24733

483 Strickland, D., X. Yao, G. Gawlak, M. K. Rosen, K. H. Gardner and T. R. Sosnick (2010). "Rationally
484 improving LOV domain-based photoswitches." Nat Methods **7**(8): 623-626.10.1038/nmeth.1473

485 Subach, F. V. and V. V. Verkhusha (2012). "Chromophore transformations in red fluorescent proteins."
486 Chem Rev **112**(7): 4308-4327.10.1021/cr2001965

487 Sun, W., W. Zhang, C. Zhang, M. Mao, Y. Zhao, X. Chen and Y. Yang (2017). "Light-induced protein
488 degradation in human-derived cells." Biochem Biophys Res Commun **487**(2): 241-
489 246.10.1016/j.bbrc.2017.04.041

490 Talia, S. D., J. M. Skotheim, J. M. Bean, E. D. Siggia and F. R. Cross (2007). "The effects of molecular
491 noise and size control on variability in the budding yeast cell cycle." Nature **448**(7156): 947-
492 951.10.1038/nature06072

493 Tautz, D. (2000). "Evolution of transcriptional regulation." Current opinion in genetics & development
494 **10**(5): 575-579

495 Teste, M.-A., M. Duquenne, J. M. François and J.-L. Parrou (2009). "Validation of reference genes for
496 quantitative expression analysis by real-time RT-PCR in Saccharomyces cerevisiae." BMC molecular
497 biology **10**(1): 99

498 Toettcher, J. E., D. Gong, W. A. Lim and O. D. Weiner (2011). "Light-based feedback for controlling
499 intracellular signaling dynamics." Nature methods **8**(10): 837

500 Uhlendorf, J., A. Miermont, T. Delaveau, G. Charvin, F. Fages, S. Bottani, G. Batt and P. Hersen (2012).
501 "Long-term model predictive control of gene expression at the population and single-cell levels."
502 Proceedings of the National Academy of Sciences **109**(35): 14271-14276

503 Varshavsky, A. (2008). "Discovery of cellular regulation by protein degradation." Journal of Biological
504 Chemistry **283**(50): 34469-34489

505 Vogel, C. and E. M. Marcotte (2012). "Insights into the regulation of protein abundance from proteomic
506 and transcriptomic analyses." Nature Reviews Genetics **13**(4): 227

507 Wachter, R. M. (2007). "Chromogenic cross-link formation in green fluorescent protein." Accounts of
508 chemical research **40**(2): 120-127

509 Zilfou, J. T. and S. W. Lowe (2009). "Tumor suppressive functions of p53." Cold Spring Harbor
510 perspectives in biology **1**(5): a001883

511

512